Electric-field gradients at the ^{111}In and ^{111m}Cd sites in undoped and Mg-doped $LiNbO_3$

B. Hauer* and R. Vianden
Institut für Strahlen- und Kernphysik, Nussallee 14-16, D-53115 Bonn, Germany

J. G. Marques and N. P. Barradas
Centro de Física Nuclear da Universidade de Lisboa, Avenida do Professor Gama Pinto 2, P-1699 Lisboa Codex, Portugal

J. G. Correia
Centro de Física Nuclear da Universidade de Lisboa, Avenida do Professor Gama Pinto 2, P-1699 Lisboa Codex, Portugal and Particle Physics Experiments Division, CERN, CH-1211 Geneva 23, Switzerland

A. A. Melo and J. C. Soares
Centro de Física Nuclear da Universidade de Lisboa, Avenida do Professor Gama Pinto 2, P-1699 Lisboa Codex, Portugal

F. Agulló-López and E. Dieguez
Departamento de Física de Materiales, C-IV, Universidad Autonoma de Madrid, Cantoblanco, 28049 Madrid, Spain
(Received 4 August 1994)

The quadrupole interaction of ^{111}Cd in undoped (congruent) and Mg-doped $LiNbO_3$ single crystals has been studied using the perturbed angular correlation technique after implantation of ^{111}In and ^{111m}Cd. A stepwise-annealing procedure shows the lattice to be fully reconstructed at 773 K. Our results show that both In and Cd are in the Li position. Mg doping at 6 mol % does not have any effect on the lattice location of these impurities in $LiNbO_3$.

I. INTRODUCTION

The possibility to control the optical properties of a material by applying electric fields or illuminating it with light opened many applications in the fields of optical signal processing, telecommunications, and optical display or storage devices. $LiNbO_3$, due to its high electro-optic coefficients, transparency range, and the availability of large and good quality single crystals, is one of the most promising materials for bulk and waveguide optoelectronic devices.[1] Furthermore, a large number of potential applications to information storage and real-time holography relies on its photorefractive behavior.[2]

It is known that the optical properties of $LiNbO_3$ can be influenced by doping the material with metal impurities.[3] Transition metals (e.g., Mn, Fe) increase the photorefractive sensitivity, Ti diffusion leads to excellent optical waveguides, and $LiNbO_3$ doped with rare-earth ions is a promising laser material. The importance of Mg-doping is derived from the reported hundredfold increase in the resistance against optical damage.[4] However, up to now the underlying mechanisms and, in many cases, even the lattice site on which the impurities are incorporated were not known. Recently the lattice sites of the important doping ions Fe and Ti were determined,[5–7] and contrary to widespread assumptions it turned out that both impurities occupy the Li instead of the Nb site. In contrast, Hf occupies Li sites in undoped $LiNbO_3$ and Nb sites in Mg-doped $LiNbO_3$.[8]

Knowledge of the lattice environment of dopants is essential for the theoretical understanding of the impurity effects as well as for any predictions about the location of energy levels and electron or hole trapping capabilities. In the present study we applied the structurally sensitive perturbed angular correlation (PAC) method[9] to the study of the incorporation of implanted In and Cd into the $LiNbO_3$ lattice with and without Mg doping.

II. EXPERIMENTAL DETAILS

The PAC technique probes the interaction between the nuclear quadrupole moment of a suitable nucleus and the electric-field gradients (EFG) produced by the surrounding electric charges, e.g., the ions of a crystal lattice. Due to its symmetry properties, the EFG tensor vanishes if the charge symmetry about a particular site is of cubic or higher symmetry. Since the EFG drops with the cube of the distance from the generating charge, only deviations from a perfect cubic symmetry in the first- and second-nearest-neighbor shell surrounding the probe nucleus lead to measurable effects. Thus, the PAC technique is an ideal tool for the study of the microscopic lattice surrounding of impurities (dopants), which yields information about the presence and position of defects in the vicinity of the probes and/or small displacements of the probe atoms from the ideal lattice position.

The PAC probe has to be an unstable nucleus, decaying via a γ-γ cascade. The probe ^{111}Cd used in the present study was obtained either via electron capture decay of implanted ^{111}In, or directly by implantation of the metastable state ^{111m}Cd. The corresponding decay schemes are shown in Fig. 1. Due to the conservation of angular momentum the emission directions of the γ rays

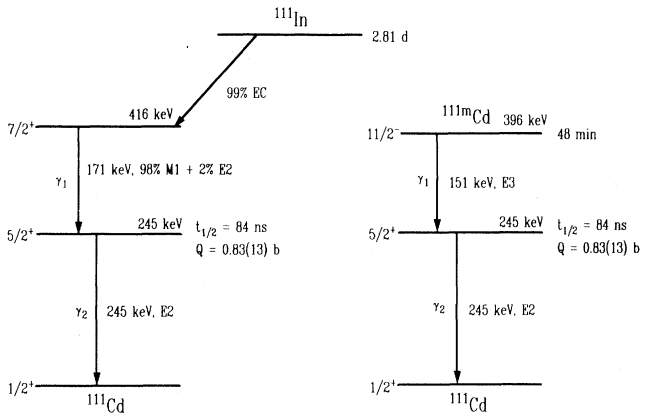

FIG. 1. Partial decay scheme of the PAC probe nuclei ^{111}In and ^{111m}Cd.

populating and depopulating the intermediate nuclear state of ^{111}Cd are correlated. This correlation is changed by a quadrupole interaction between the quadrupole moment of the nucleus in the intermediate state and an EFG. The interaction leads to a modulation of the angular correlation pattern depending on the time spent in the intermediate state.

The 171–245 keV cascade from the decay of ^{111}In was used for γ-γ PAC experiments and the 151–245 keV cascade from the decay of the ^{111m}Cd was used for e^--γ experiments, taking advantage of this significant conversion coefficient for the K electrons from the 151-keV transition, $\alpha_K = 1.5$.[10] The 245-keV intermediate state common to both cascades has a spin $I = \frac{5}{2}$, a half-life of $T_{1/2} = 84$ ns, and a quadrupole moment of $|Q| = 0.81(13)b$.[11] The half-lives of the implanted mother isotopes are quite different, 2.83 days for ^{111}In and 48.6 m for ^{111m}Cd. Therefore systematic studies on lattice recovery after implantation were performed only with ^{111}In. The final results obtained with both systems are directly comparable since the intermediate state of the cascade is the same. The only difference is in the value of the anisotropy, which is $A_{22} = -0.178$ for the γ-γ cascade of In and $A_{22} = +0.230$ for the e^--γ cascade of Cd.[12] Details of the application of the PAC technique can be found in the literature.[13]

Congruent $LiNbO_3$ crystals, [Li]/[Nb]=0.945, were grown under oxygen atmosphere in the Crystal Growth Laboratory of the "Universidad Autonoma de Madrid" by the Czochralski method from grade I Johnson-Matthey powder. Crystals doped with 6 mol % Mg were also grown. Plates were cut both perpendicular and parallel to the c axis, polished with 0.3-mm alumina powder, and cleaned with ethanol.

Commercially available ^{111}In dissolved in 0.1N HCl was dried in the source of the Bonn University isotope separator and subsequently evaporated and ionized. The In ions were then accelerated to an energy of 150 keV and implanted into the pure $LiNbO_3$ samples to doses of 1×10^{13} at./cm^2, with the main dose fraction ($>90\%$) being due to unavoidable stable Cd contamination. A mean range of 70 nm for 150-keV In ions was calculated with the TRIM code,[14] with a maximum volume concentration of 2×10^{18} In/cm^3.

The γ-γ PAC measurements were carried out with a four-detector setup equipped with BaF_2 scintillators. They were arranged in a plane forming 90° between adjacent detectors. The shape of the scintillators (cut cones) and their distance of typically only 10 mm to the sample ensured large solid angles and thus a good efficiency of the setup. The excellent timing properties of the setup[15] allowed a time resolution of 0.3 ns (FWHM) for the ^{111}In cascade.

The implantation of ^{111m}Cd was carried out at the ISOLDE mass separator at CERN.[16] The Cd isotope was produced by the spallation reaction of a 1-GeV proton beam on a molten Sn target. The isotopes were ionized in a discharge plasma ion source and the Cd ions then extracted and accelerated electrostatically to an energy of 60 keV. After mass separation the ^{111m}Cd ions were implanted into undoped and Mg-doped $LiNbO_3$ samples to a dose of 5×10^{12} at./cm^2. The mean range of the ions is 40 nm, with a maximum concentration of 1×10^{18} Cd/cm^3.

The e^--γ PAC experiments were performed using a setup consisting of two β spectrometers of the Siegbahn type[17] and two BaF_2 detectors. The electromagnetic lenses and the γ detectors were arranged in a plane and their position relative to each other is such that each lens makes 90° with one γ detector and 180° with the other. The time resolution of this setup was 1.0 ns (FWHM) for the ^{111m}Cd cascade.

Delayed coincidence spectra $N(\theta,t)$ were recorded automatically in both cases for the interdetector angles of $\theta = 90°$ and 180°. From these spectra the time differential anisotropy

$$R(t) = 2[N(180°,t) - N(90°,t)]/[N(180°,t) + 2\times N(90°,t)]$$

was calculated.

In the case of an intermediate state with a spin $I = \frac{5}{2}$ the time-differential anisotropy can be described by the product of the anisotropy A_{22} of the cascade and the so-called perturbation factor $G_{22}(t)$. This function contains the information about the quadrupole interaction and has the form

$$G_{22}(t) = \sum_{n=0}^{3} s_n \cos[c_n(\eta)\nu_Q t] \exp -[\delta^2 c_n(\eta)\nu_Q t] \ . \quad (1)$$

The quadrupole constant $\nu_Q = eQV_{zz}/h$ and the asymmetry parameter $\eta = (V_{xx} - V_{yy})/V_{zz}$, which can be deduced from the frequency factors, contain information about the magnitude of the principal component V_{zz} and the asymmetry of the EFG, respectively. The exponential factor allows for a Gaussian distribution of EFG's around a mean value. Such a distribution can be caused, e.g., by different lattice defects in the vicinity of the probe atoms. The s_n coefficients can be calculated for polycrystalline as well as single-crystalline samples as in the present case.[18] If fractions f_i of the total number of ra-

dioactive probes are in different but unique sites experiencing different EFG's the observed spectra might be described by the sum over several perturbation functions $f_i \cdot G^i_{22}(t)$ with the sum of the f_i normalized to one.

The annealing of the lattice damage caused by the implantation and the incorporation of the probe atoms into the undisturbed crystal lattice was studied in an isochronous annealing program. The samples implanted with ^{111}In were heated in air to temperatures between 573 and 973 K, kept there for 30 min, and cooled slowly back to the measuring temperature of 293 K. Spectra for sample temperatures below room temperature were taken by mounting the sample on the second stage of a closed-cycle refrigerator and adjusting it to the desired temperature between 293 and 15 K. The sample implanted with ^{111m}Cd was annealed at 873 K in air for 30 min and slowly cooled to the measuring temperature of 293 K.

III. RESULTS

A. ^{111}In in undoped $LiNbO_3$

In Fig. 2, the PAC spectra obtained with ^{111}In in undoped $LiNbO_3$ before the first and after the last annealing step at 970 K are shown. As is evident from the lack of structure in Fig. 2(a), the implantation has led to a complete destruction of the lattice in the vicinity of the probe atoms. All the In probes ($f_1 = 1.0$) are therefore subjected to large nonunique EFG's. A least-squares computer program adjusted the parameters of Eq. (1) to fit the data and yielded a broad distribution of quadrupole interaction frequencies centered at $\nu_Q = 185(2)$ MHz and a relative width $\delta = 0.34$.

The isochronous annealing led to the gradual appearance of a periodic structure in the PAC spectra [Fig. 2(b)], indicating that the lattice is reconstructed and the In probes are incorporated on well-defined lattice positions. Assuming that the In probes are in a unique configuration, they would experience only a unique EFG. Due to the symmetry properties of the $LiNbO_3$ lattice, the EFG expected at the most probable lattice sites of Li or Nb, as well as the ideal octahedral interstitial site, has axial symmetry, i.e., $\eta = 0$. However, attempts to fit the data with only one quadrupole interaction frequency and $\eta = 0$ led to unsatisfactory results. Besides, Fourier analyses of the spectra showed an asymmetric line indicating the presence of a second frequency with a value only slightly higher than the main component. Therefore, two unique, axially symmetric probe configurations were assumed and indeed this greatly improved the quality of the fit. The adjusted parameters of Eq. (1) for the two fractions f_2 and f_3 are shown in Fig. 3. The EFG's corresponding to ν_{Q2} and ν_{Q3} differ by only about 5%.

As can be seen in Fig. 3, the fractions f_2 and f_3 build up rapidly around 700 K as the $LiNbO_3$ lattice is reconstructed. As a consequence of this isochronous annealing study, for all further investigations a two-step annealing, 30 min at 623 K and 30 min at 823 K in air, was adopted.

In order to verify the assumed orientation of the principal component V_{zz} of the EFG's, PAC measurements

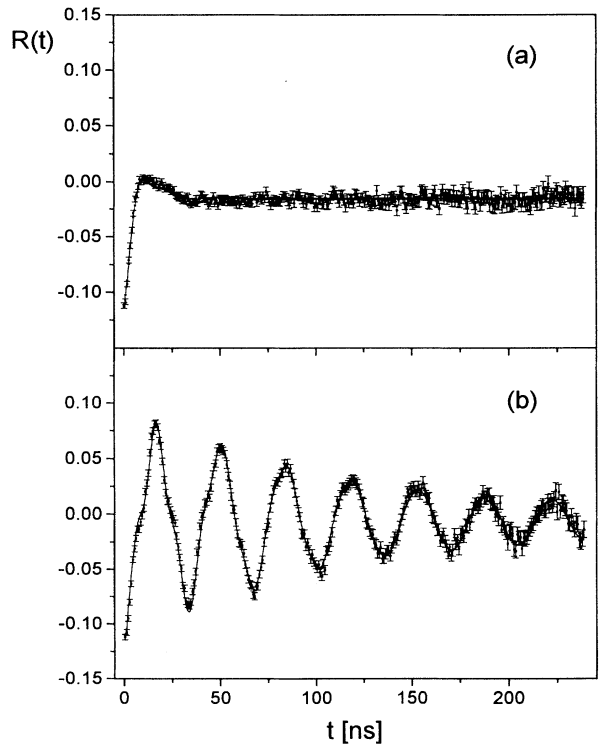

FIG. 2. Time-dependent anisotropy of the 172–245 keV γ-γ cascade of ^{111}In(^{111}Cd) in undoped $LiNbO_3$ as implanted (a) and after annealing of the sample for 30 min at 970 K (b).

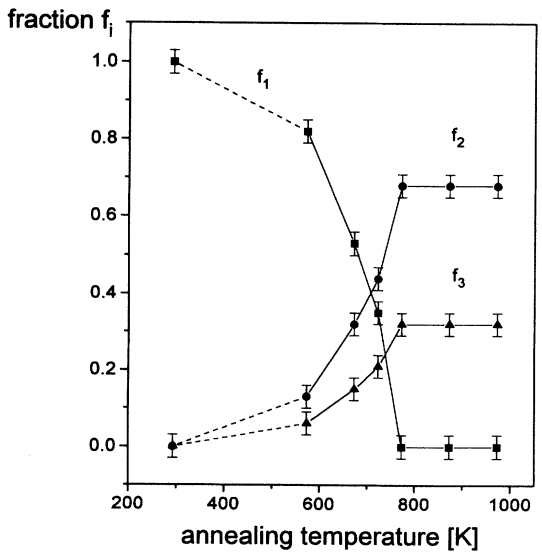

FIG. 3. Fractions of ^{111}In in damage associated sites (f_1) and two unique lattice sites (f_2,f_3) immediately after the implantation (leftmost points) and after annealing for 30 min at each of the indicated temperatures.

TABLE I. Values of the quadrupole interaction of ^{111}In in congruent $LiNbO_3$ as derived from a least-squares fit to the data.

^{111}In(^{111}Cd)	ν_Q (MHz)	η	δ	f
Site 1	192(1)	0.11(2)	0.028(3)	0.68(3)
Site 2	205(1)	0.16(4)	0.044(5)	0.32(3)

were carried out for different orientations of the $LiNbO_3$ single crystal with respect to the detector setup. Two main geometries were chosen corresponding to an alignment of the c axis with the normal of the detector plane (I) and with the angle bisector of the two detectors forming an angle of 90° (II). For V_{zz} parallel to c in geometry (I), s_1 in Eq. (1) would be the dominant coefficient with s_2 and s_3 nearly vanishing, whereas in geometry (II) s_1 and s_2 are roughly equal with s_3 still being small. The corresponding PAC spectra are shown in Fig. 4. Clearly for geometry II a second component with $c_2(\eta) \sim 2c_1(\eta)$ is present. A fit of the theoretical perturbation function indeed yielded the result expected for an alignment of the principal component V_{zz} of both EFG's with the c axis of the $LiNbO_3$ lattice. It should be mentioned that these extremely accurate results also unambiguously confirm the presence of two closely spaced frequencies in the spectra as discussed above.

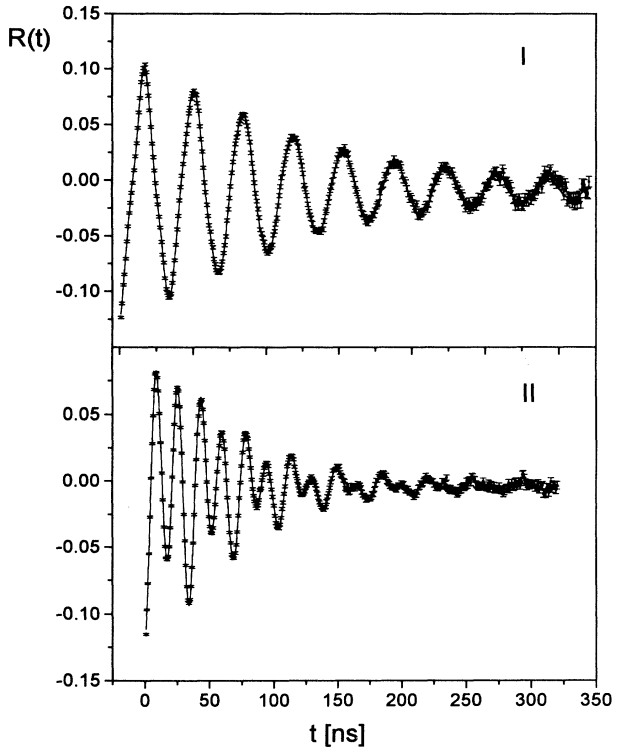

FIG. 4. Time-dependent anisotropy of the 172–245 keV γ-γ cascade of ^{111}In(^{111}Cd) in undoped $LiNbO_3$ after annealing of the sample for 30 min at 973 K for different orientations of the c axis of the $LiNbO_3$ single crystal relative to the PAC detectors: (a) c normal to the detector plane, (b) c aligned with the angle bisector of two detectors under 45°.

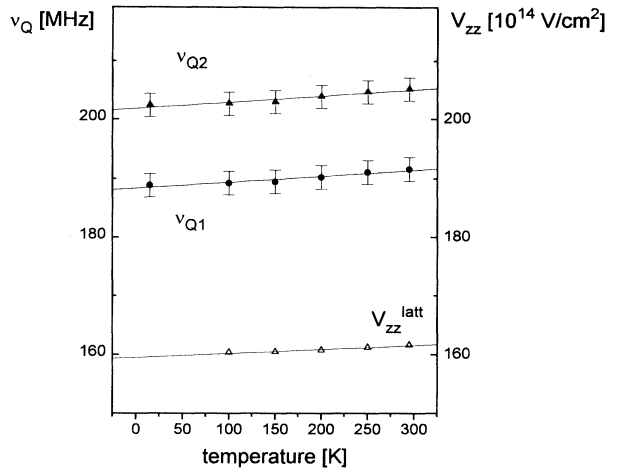

FIG. 5. Variation of ν_{Q1} and ν_{Q2} with the sample temperature. For comparison the EFG value V_{zz}^{latt} calculated in the point charge model (see text) for the corresponding lattice parameters is shown in the lower part.

Further, although the EFG on the ideal lattice site should have axial symmetry, it was observed that allowing for a small η improved the quality of the fit considerably. Since η is strongly correlated with the width of the frequency distribution δ,[19] it was tested if a similar improvement could be achieved by varying δ. Since this attempt failed, in a next step the asymmetry parameter η was varied stepwise for each fraction. The lowest χ^2 value for the fits were achieved for $\eta_1 = 0.11(2)$ and $\eta_2 = 0.16(4)$ together with the parameter values given in Table I.

Cooling the sample led to only very slight variations of the quadrupole interaction frequencies. The resulting fit values are shown in Fig. 5.

B. ^{111m}Cd in undoped and Mg-doped $LiNbO_3$

Taking into account the results from the annealing sequence described in the previous section, only one annealing step was performed at 873 K. In Fig. 6, the PAC

TABLE II. Values of the quadrupole interaction of ^{111}Cd in undoped and Mg-doped $LiNbO_3$ as derived from a least-squares fit to the data. The η values have been kept fixed to the ones given in Table I.

^{111m}Cd(^{111}Cd)		ν_Q (MHz)	η	δ	f
Mg doped	Site 1	191(2)	0.11	0.035(5)	0.68(5)
	Site 2	204(2)	0.16	0.035(5)	0.32(5)
Undoped	Site 1	192(2)	0.11	0.027(5)	0.71(5)
	Site 2	205(2)	0.16	0.038(5)	0.29(5)

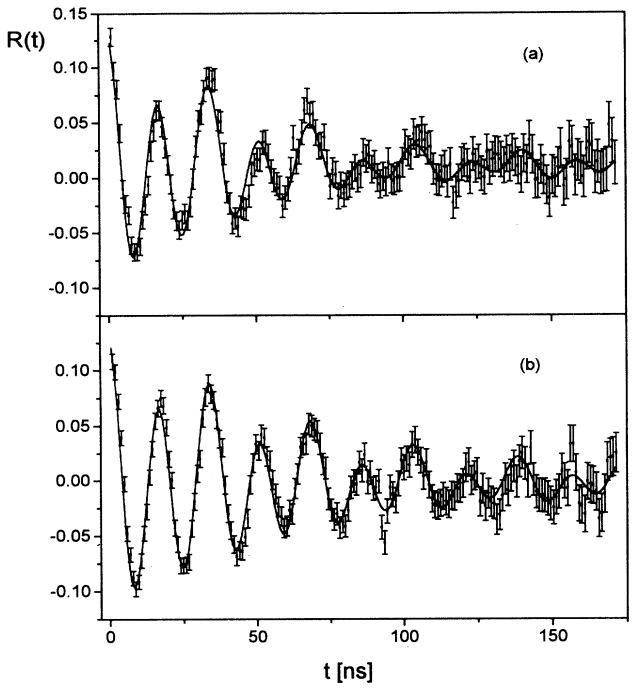

FIG. 6. Time-dependent anisotropy of the 151–245 keV γ-γ cascade of ^{111}Cd(^{111}Cd) after annealing for 30 min at 970 K in Mg-doped (a) and undoped $LiNbO_3$ (b).

spectra obtained with ^{111m}Cd in undoped [Fig. 6(a)] and Mg-doped $LiNbO_3$ [Fig. 6(b)] after annealing are shown, for geometry (II). Obviously apart from a slightly different damping there are no differences among the interaction patterns in both cases. Further they are also very similar to the results obtained for ^{111}In, except for the opposite sign of the anisotropy (seen at $t=0$ ns). The same frequencies are observed in the corresponding Fourier transforms. Consequently, the same model function was fitted to the data. Due to the lower statistics, in the least-squares fit of the spectrum obtained after annealing at 873 K, the values of η for the two sites were kept fixed at the ^{111}In values. The final results are given in Table II. The values obtained for the two fractions agree within error bars with the ones obtained for ^{111}In.

IV. DISCUSSION OF THE RESULTS

Since independently of the parent activity the intermediate state of the probe nucleus for the three experiments described in Sec. III is the same it is possible to directly compare the results obtained in both systems. Therefore, considering that the measured quadrupole interaction frequencies, i.e., the hyperfine fields at the probe sites, are the same, one can conclude that the In and Cd probes occupy sites with identical lattice environments. In a similar way it can be argued that, since the presence of Mg does not lead to any observable change in the frequencies (see Tables I and II), its presence at a 6 mol % concentration has no influence on the lattice site of ^{111m}Cd. The lattice site of In in Mg-doped $LiNbO_3$ was recently determined by the PIXE/channeling technique to be the Li site.[20] Since presently in all known cases[8,21] an increase of the Mg concentration could induce only a shift of an impurity from the Li site to the Nb site, the location of In on the Li site in Mg-doped $LiNbO_3$ implies the same site for In in undoped $LiNbO_3$. Therefore it can be concluded that also Cd in undoped and Mg-doped $LiNbO_3$ occupies the Li site.

The two fractions observed in this work, f_2 and f_3, are likely to correspond to the same Li location, since even a 30% occupancy of a second site would have led to pronounced effects in the RBS-channeling results cited above. Therefore the small difference in the EFG, only $\sim 5\%$, is most probably due to the presence of a defect in the vicinity of one fraction of probe nuclei whereas the other fraction resides in a perfect lattice environment. The defect is not likely to be a Nb_{Li} (Nb antisite), always present in congruent $LiNbO_3$, since Mg is known to substitute Nb in this position[21,22] and no change in the relative values of the two fractions is observed between Mg-doped and undoped material.

The most probable defect to be trapped at the In_{Li} impurity is a Nb vacancy. Nb vacancies are always present in $LiNbO_3$ and the difference in their concentration between undoped and Mg-doped (6 mol %) is small.[21] It should be mentioned that two, three, and even four slightly different values have been observed for the frequencies of optical transitions in some rare-earth dopants.[23–25] Similar to our suggestion, the effect of close-by intrinsic defects has been invoked to account for this behavior.

Unfortunately the influence of such a defect on the EFG at the probe site cannot be reliably calculated up to now. Successful EFG calculations have only been carried out for pure, noncubic metals using the linearized-augmented-plane-wave method.[26] Therefore we used the rather simple point charge model of De Wette[27] to obtain a theoretical estimate for the EFG in an undisturbed $LiNbO_3$ lattice and the changes produced by a Nb vacancy in an adjacent Nb site on the c axis. Although this model, which takes into account only the ions of the lattice (except for assuring the charge neutrality the electrons are neglected) has been quite successful in predicting the symmetry, the orientation and relative changes in the EFG whereas the absolute values for V_{zz} are usually not well reproduced. For the In_{Li} site such a calculation yields an axially symmetric ($\eta=0$) EFG of $V_{zz}^{\text{latt}}=+0.1616\times10^{17}$ V/cm^2 at $T=293$ K with the principal component oriented along the c axis ($\langle 0001 \rangle$). Except for the absolute value of V_{zz}^{latt} and the small deviation in η this is in good agreement with the experimental result (see Table III). Further the introduction of a Nb vacancy in the next-nearest Nb octahedron leads to a reduction of the EFG at the In_{Li} site.

The same model was used to estimate the influence of temperature-induced changes in the lattice parameters on the EFG. As can be seen in Fig. 5, the weak trend observed for the quadrupole interaction frequencies, a de-

TABLE III. Parameters of the quadrupole interaction, quadrupole moments (Ref. 10) and derived absolute values of the EFG for different PAC probes in $LiNbO_3$. The errors quoted for V_{zz}^{latt} include the errors of the quadrupole interaction frequencies and moments but not that of the theoretically calculated Sternheimer factors, taken from Sen *et al.* (Ref. 30) for Sc and Feiock and Johnson (Ref. 29) for Ta (interpolated) and Cd.

PAC probe	^{44}Sc (^{44}Ti)	^{181}Ta (^{181}Hf)	^{111}Cd(^{111}In/^{111m}Cd)	
ν_Q (MHz)	15.4(2)	1184(16)	191.2	201.6
η	0.14(−)	0.235(25)	0.13	0.11
Orientation	⟨0001⟩	⟨0001⟩	⟨0001⟩	
$\lvert Q\rvert$ (b)	0.21(2)	2.53(10)	0.83(13)	
$\lvert V_{zz}^{eff}\rvert$ (10^{17} V/cm^2)	3.0(3)	19.4(8)	9.54(1.5)	10.06
$(1-\gamma_\infty)$	11.4	62	30.3	
$\lvert V_{zz}^{latt}\rvert$ (10^{17} V/cm^2)	0.27(3)	0.31(2)	0.31(5)	0.33(5)

crease with decreasing temperature, is well reproduced by the EFG calculated with the lattice parameters for these temperatures.[1]

Since various other impurities were found to occupy the Li site[6,7] and In has the same covalent radius as Hf ($r=0.144$ nm), which also has been shown to occupy the Li site,[5] it is interesting to compare the EFG's measured with the different PAC probes ^{44}Sc, ^{111}Cd, and ^{181}Ta on this site. Experimentally an effective EFG of $3.0(3)\times10^{17}$ V/cm^2 and $19.6(1.5)\times10^{17}$ V/cm^2 was derived for ^{44}Sc and ^{181}Ta, respectively.[7,28] The corresponding value for ^{111}Cd is $9.5(1.5)\times10^{17}$ V/cm^2. In all cases the error is mostly due to the uncertainty in the quadrupole moments (see Table III). After correcting for the influence of the probe's own electron shell by dividing by the so-called Sternheimer antishielding factor[29] a remarkable similarity of V_{zz}^{latt} is observed (Table III). This can be taken as further support of the site assignment made above.

However, in all previous and also in the present measurements the fits to the data always yielded a small axial asymmetry of the EFG with η ranging from 0.11 to 0.23. This problem has been addressed by Hauer *et al.*[7] and it was suggested that possibly the presence of a lattice defect near the probe atoms in an off c-axis position could be responsible for this deviation from axial symmetry. A further possibility should be mentioned here: Similar to the present situation an axial symmetry has been observed for ^{181}Hf in Hf metal although this has an ideal hcp structure where no η is expected.[31] There this effect was attributed to the presence of small amounts (1–5 at. %) of a Zr impurity and vanished in pure Hf crystals. It could be possible that, e.g., the presence of the Nb vacancies, also at a level of a few percent could cause a similar effect. Measurements in stoichiometric $LiNbO_3$ crystals where the amount of Nb vacancies is much lower could help to clarify this interesting effect.

V. CONCLUSIONS

The EFG at the In and Cd sites in pure and Mg-doped $LiNbO_3$ was investigated by the PAC technique. It could be concluded that both impurities, In and the Cd, occupy the Li site in the $LiNbO_3$ lattice. The presence of the codopant Mg up to 6 mol % does not change the lattice site of these elements, indicating that In and Cd seem to behave similar to Mg. It is interesting to note that this conclusion is strongly supported by a recent investigation of Volk and Rubinina[32] where it was found that In impurities increase the resistance of $LiNbO_3$ to optical damage much like Mg and Zn. The temperature dependence of the EFG is mainly due to changes in the lattice parameters. The EFG at the Li site seems to be rather independent of the impurity. In all cases a small axial asymmetry of the EFG was observed, although the lattice symmetry at the Li site predicts axial symmetry. It is suggested that this effect is due to the influence of the considerable concentration of Nb vacancies in congruent $LiNbO_3$.

ACKNOWLEDGMENTS

This work was partially funded by INIDA (Germany), the BMFT through the KFZ Karlsruhe, and JNICT (Portugal). J.G.M. and N.P.B. thank JNICT for grants under the CERN and CIENCIA programs. We gratefully acknowledge the support of the ISOLDE Collaboration (PPE division, CERN, Geneva).

*Present address: Institut für Festkorperforschung, Forschungszentrum Jülich, D-52425 Jülich, Germany.

[1] *Properties of $LiNbO_3$*, EMIS Data Reviews Series No. 5 (INSPEC, London, 1989).

[2] *Photorefractive Materials and Their Applications*, edited by P. Gunther and J. P. Huigard (Springer-Verlag, Berlin, 1988), Vols. 1 and 2.

[3] R. C. Alferness, Science **234**, 825 (1986), and references cited therein.

[4] D. A. Bryan, R. Gerson, and H. E. Tomascheke, Appl. Phys. Lett. **44**, 847 (1984).

[5] L. Rebouta, M. F. da Silva, J. C. Soares, M. Hage-Ali, J. P. Stoquert, P. Siffert, J. A. Sanz-Garcia, E. Dieguez, and F. Agulló-Lopez, Europhys. Lett. **14**, 557 (1991).

[6] D. Kollewe, A. Kling, B. C. Grabmeier, T. Bremer, W. Heiland, and W. Zimmermann, Phys. Lett. A **169**, 77 (1992).

[7] B. Hauer, R. Vianden, M. F. da Silva, L. Rebouta, J. C. Soares, E. Dieguez, and F. Agulló-López, J. Phys. Condens. Matter **6**, 267 (1994).

[8] L. Rebouta, P. J. M. Smulders, D. O. Boerma, F. Agulló-Lopez, M. F. da Silva, and J. C. Soares, Phys. Rev. B **48**, 3600 (1993).

[9] R. M. Steffen and K. Alder, in *The Electromagnetic Interaction in Nuclear Spectroscopy*, edited by W. D. Hamilton (North-Holland, Amsterdam, 1975).

[10] *Table of Isotopes*, 7th ed., edited by C. M. Lederer and V. S. Shirley (Wiley, New York, 1978).

[11] P. Herzog, K. Freitag, M. Reuschenbach, and H. Walitzi, Z. Phys. A **294**, 13 (1980).

[12] R. S. Hager *et al.*, Nucl. Data Tables A **4**, 397 (1968).

[13]R. Vianden, *Impurity-Defect Interaction in Metals,* Vol. 144 of *NATO Advanced Study Institute, Series E* (Kluwer-Academic, Dordrecht, 1988), p. 239.
[14]J. P. Biersack and L. G. Haggmark, Nucl. Instrum. Methods **174**, 257 (1980).
[15]Th. Schaefer, Ph.D. thesis, University of Bonn, 1992.
[16]E. Kugler, D. Fiander, B. Jonson, H. Haas, A. Przewloka, H. L. Ravn, D. J. Simon, and K. Zimmer, ISOLDE Collaboration, Nucl. Instrum. Methods B **70**, 41 (1992).
[17]P. Kleinheinz, L. Samuelsson, R. Vucanovic, and K. Siegbahn, Nucl. Instrum. Methods **32**, 1 (1965).
[18]D. Wegner, Hyperfine Interact. **23**, 179 (1985).
[19]M. Forker, Nucl. Instrum. Methods **106**, 121 (1973).
[20]L. Kovács, L. Rebouta, J. C. Soares, M. F. da Silva, M. Hage-Ali, J. P. Stoquert, P. Siffert, C. Zaldo, Zs. Szaller, and K. Polgar, Mater. Sci. Eng. B **9**, 505 (1991).
[21]O. F. Schirmer, O. Thiemann, and M. Wöhlecke, J. Phys. Chem. Solids **52**, 185 (1991).
[22]L. J. Hu, Y. H. Chang, F. S. Yen, S. P. Lin, I-Nan Lin, and W. Y. Lin, J. Appl. Phys. **69**, 7635 (1991).
[23]J. Garciá-Solé, T. Petit, H. Jaffrezik, and G. Boulon, Europhys. Lett. **24**, 719 (1993).
[24]A. Lorenzo, L. E. Bausá, and J. Garciá-Solé, J. Phys. Condens. Matter **6**, 1 (1994).
[25]R. Duchowicz, L. Nuñez, J. O. Tocho, and F. Cussó, Solid State Commun. **88**, 439 (1993).
[26]P. Blaha, K. Schwarz, and K. Dederichs, Phys. Rev. B **37**, 2792 (1988).
[27]F. De Wette and G. E. Schacher, Phys. Rev. **137**, A92 (1965).
[28]L. Rebouta, J. C. Soares, M. F. da Silva, J. A. Sanz-Garcia, E. Dieguez, and F. Agulló-López, Nucl. Instrum. Methods B **45**, 495 (1990).
[29]F. D. Feiock and W. R. Johnson, Phys. Rev. **187**, 39 (1969).
[30]K. D. Sen, P. Weiss, and P. C. Schmidt, Hyperfine Interact. **30**, 253 (1986).
[31]R. L. Rasera, T. Butz, A. Vasquez, H. Ernst, C. K. Shenoy, B. D. Dunlap, R. C. Reno, and G. Schmidt, J. Phys. F **8**, 1579 (1978).
[32]T. R. Volk and N. M. Rubinina, Ferroelectric Lett. **14**, 37 (1992).